

# Evaluation of horizontal and vertical queueing models in relation to observed trajectory data in a signalized urban traffic network

Leah Anderson (corresponding author)  
University of California, Berkeley  
California PATH  
3 McLaughlin Hall  
Berkeley, CA 94720-1720  
phone: (415)827-6061,  
leah.anderson@berkeley.edu

Gabriel Gomes  
University of California, Berkeley  
California PATH  
3 McLaughlin Hall  
Berkeley, CA 94720-1720  
gomes@path.berkeley.edu

Alexandre M. Bayen  
University of California, Berkeley  
California PATH  
3 McLaughlin Hall  
Berkeley, CA 94720-1720  
bayen@berkeley.edu

Paper submitted to TRB Annual Meeting 2015  
November 12, 2014

214 words in abstract + 4450 words in text + 8 figures + 1 table  
with 34 references  
⇒ Total word count: 6936 / 7000

**ABSTRACT**

While the Cell Transmission Model (CTM) is generally accepted as a standard representation of traffic flows on freeways with long links and uninterrupted flows, less is known about the accuracy of CTM or other macroscopic queueing models on urban road networks with short links and frequent flow blockages due to signal control. In fact, almost all existing validations of CTM focus on modeling freeways. In this paper, we aim to provide evidence towards selecting the appropriate queueing model dynamics for use in analysis and control of a large-scale network of signalized traffic intersections. We introduce a new vertical queueing dynamics called the Vertical Cell Model (VCM) that incorporates a representation of link transit time and finite queue capacity. The linear link model of VCM provides an attractive new alternative to CTM for practical network-wide estimation and control procedures. We then compare the link outflow and density outputs of both VCM and CTM to a set of high fidelity ground-truth observations on a multi-intersection segment of an existing urban roadway. Ultimately we provide a validation of both CTM and VCM for use in arterial networks which have minimal observed over-saturation. The development and validation of VCM is a first step toward a new control-theoretic approach to the operations of signalized intersections in a large-scale network.

## INTRODUCTION

As traffic congestion in urban areas increases while space for building new capacity depletes, many agencies responsible for local traffic management will be forced to take a deeper look into how to influence flow dynamics and improve global congestion patterns on their existing road networks. However such analysis requires the application of practical and efficient traffic models that can handle various levels of congestion and types of control. While researchers have extensively explored the idea of modeling dynamic traffic networks for more than a half century, most of the theoretical work has been more easily applied to freeways than to realistic networks of signalized urban intersections—often leaving traffic managers dependent on computationally demanding and highly parameter-sensitive microscopic traffic models for the analysis of arterial traffic networks.

The first introduction of a dynamic network-wide model for signalized roadways appears to have come from Gazis et al. (1, 2), which introduces a discrete-time *store and forward* model of flows between controlled intersections for the purposes of delay-minimizing optimal control. This form of *vertical queueing model* introduces a representation of a road network as a graphical model in which vehicles are passed between intersection “nodes” along road “links” at each time step. The characteristics of the modeling framework were highly limiting as they were originally proposed, yet many researchers soon published extensions of this type of model (3, 4, 5, 6). Notably, Michalopoulos and Stephanopoulos (7) made the model more applicable to flows in congested regimes by introducing the idea of transmission limitations due to finite link storage capacities.

A major shift occurred when the community appealed for the inclusion of a “fundamental diagram”, or an underlying relationship between traffic density and the modeled flow rate. This idea derives from the work of Lighthill and Whitham (8) and Richards (9), commonly known as the LWR model, in which traffic flows were modeled as hydrodynamic waves. It was believed that this step towards *horizontal queueing models* would better represent the effects of sharp density shockwaves (frequent “stop and go” behaviors) due to signal controllers (10).

The widely-adopted finite difference scheme of Daganzo known as the *Cell Transmission Model* (CTM) uses a simplified peicewise-linear fundamental diagram to provide a convergent approximation to the LWR model (11, 12). Field data suggests that CTM closely fits observations of flows on freeways or highways with few interruptions (13, 14), yet to our knowledge validation of CTM on real arterial networks with short signalized intersections is very limited. One existing numerical comparison of CTM to a vertical queueing model on an artificial grid network is presented in (15).

In recent years, CTM has been considered by many researchers to be the standard in macroscopic modeling of traffic flows. It has been used to design many traffic controllers for freeways (16), and has even been adopted in version 13 of the widely-used traffic optimization package TRANSYT (17). An analysis of the dynamic properties of CTM for use in control is provided in (18). Recently, there have been many algorithms proposed for optimal intersection signal control schemes based on the analytical dynamics of CTM (19, 20, 21, 22, 23). It is still argued, however, that the complexity and high computational requirements of these CTM-based control schemes on detailed urban networks make them impractical for the real-time application for which they were designed (24). This has in turn spawned a second look at using less detailed vertical queueing dynamics to analyze global flow patterns and design model-based control (25, 26, 27).

Bolstered by similar research in the field of communications and mechanical service networks, modern vertical queueing models have introduced a variety of transit delay and congestion propagation improvements which have made them more widely applicable than those of the 1960’s

and 1970's. Recent work yields promising results for practical network-wide control algorithms based on vertical queueing models (28, 29, 30, 31, 32, 33, 34).

The objective of the current work is therefore to provide evidence towards selecting the appropriate model dynamics for use in analysis and control of a realistic large-scale network of signalized roadways. Specifically, the present article makes the following contributions:

1. We introduce the formulation of the *Vertical Cell Model* (VCM), a new implementation of a vertical queueing model that incorporates a simple representation of intra-link transit delay and finite link storage capacity,
2. We validate this model against a set of ground-truth density and flow measurements derived from high-resolution vehicle trajectory observations on a real urban traffic network, and
3. We show that VCM performs equally as well as CTM relative to these ground-truth observations.

We believe that we also contribute one of the first comprehensive validations of an implementation of CTM against high-fidelity observations on a real network of signalized intersections with short, congested links. This type of validation has been largely limited by the the lack of appropriate data on urban networks.

We ultimately seek to determine whether a horizontal queueing pattern adds significant benefit to network-wide model accuracy on a signalized traffic network with practical model time discretization. The relative analytical simplicity of the link dynamics of VCM make it an attractive option for use in model-based arterial estimation and signal control, especially if performance of VCM and CTM are proven to be comparable. To ensure fair comparison of results, we ran both models on the same computational platform using the exact same graphical network, dynamic parameters, and node model. In the future, we plan to continue to study the use of VCM for estimation and control objectives in the I-210 corridor as part of the *Connected Corridors* integrated corridor management pilot project at California PATH (<http://connected-corridors.berkeley.edu/>).

## MODEL DESCRIPTIONS

As previously mentioned, CTM and VCM share a common graphical representation of an arterial traffic network. Consider a set of short urban roads separated by signalized intersections. We model this network as a graph  $\mathcal{G} = (\mathcal{N}, \mathcal{L})$  where the set of links  $\mathcal{L}$  correspond unidirectional roadways and the set of nodes  $\mathcal{N}$  represent intersections or general points of flow division.

More specifically, each individual link  $l \in \mathcal{L}$  represents a unidirectional path between two nodes in the network with a physical capacity for vehicles to be stored. Define  $In(l)$  to be the set of all links immediately upstream of  $l$  in the network such that they can pass flow directly into  $l$  (through the node between them), and define  $Out(l)$  as the set of all links which receive a non-trivial flow directly from  $l$ .

Physical roads are typically divided into a set of *movements* corresponding to each immediate downstream destination. A movement contains to all vehicular flow on a single roadway that intends to subsequently enter the same downstream roadway at the next intersection. In this work, we consider each movement to be represented as a distinct link that is parallel to the links representing all other movements on the same roadway. These parallel links can span the entire block from upstream intersection to downstream intersection, or they can originate somewhere in

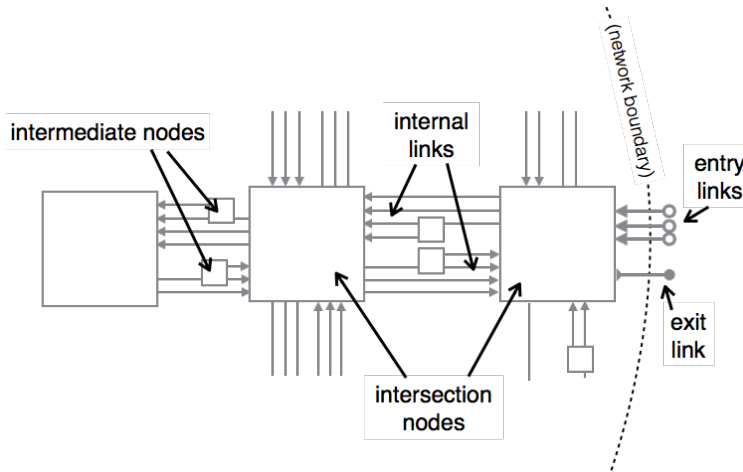


**FIGURE 1** A road network is represented by a graph containing internal links, entry links, exit links, intersection nodes, and intermediate nodes.

between two subsequent intersections at a position corresponding to the location at which a road forks into a turn pocket. This mid-link split allows for modeling of shared lanes or turn bays which can result in partial output blocking for one or more movements sharing common upstream resources.

5 The set of all links  $\mathcal{L}$  is divided into three subsets: entry links  $\mathcal{L}_{\text{entry}}$ , exit links  $\mathcal{L}_{\text{exit}}$ , and internal links  $\mathcal{L}_{\text{int}}$ . Internal links must be bounded on either side by a network node connecting them to a non-trivial set of neighboring network links. They each have finite length  $L_l$  with corresponding finite storage capacity. Therefore, the inflows and outflows of an internal link are inherently constrained by the number of vehicles on the link at any given time. Entry links originate from  
 10 outside of the network and terminate at an internal network node. Because  $In(l) = \emptyset \forall l \in \mathcal{L}_{\text{entry}}$ , demand on these links is exogenous to the network – entry links are in fact the only point of entry for external demand. For the purposes of this work, consider all time-dependent exogenous demands to be known. While there is a rate limitation on the flow exiting entry links, there is no bound on link storage; any expected demand can be stored on these links indefinitely until service  
 15 is available. In the same manner, exit links serve as an infinite repository for flow exiting the network. These links have no departing flow, and by definition  $Out(l) = \emptyset \forall l \in \mathcal{L}_{\text{exit}}$ . Yet due to an infinite storage capacity, the presence of congestion on exit links will never limit overall network outflow.

Nodes are storage-less “gateways” that govern flow between neighboring links. A node  $n \in \mathcal{N}$  is defined geometrically by its set of incoming links  $I_n$  and its set of outgoing links  $O_n$ . It is parameterized by a split ratio matrix  $\beta_n$  of dimension  $|I_n| \times |O_n|$  that defines the proportion of vehicles in each incoming link that are waiting to enter each outgoing link  $m \in Out(l)$ . Elements  $\beta_n^{l,m}$  of feasible split matrices must obey the following characteristics:

$$0 \leq \beta_n^{l,m} \leq 1 \forall l \in I_n, m \in O_n, n \in \mathcal{N} \quad (1)$$

$$\sum_{m \in O_n} \beta_n^{l,m} = 1 \forall l \in I_n, n \in \mathcal{N} \quad (2)$$

Each node in the network represents either a simple splitting of a single upstream link into many “movement” links or a point of flow exchange between two or more intersecting roadways. The topological differences between *intermediate* nodes and *intersection* nodes are illustrated in Figure 1. The operation of the intermediate nodes is straightforward: a single demand flow is consistently divided into many downstream supply flows as specified by a fixed split ratio parameter. Intersection nodes similarly split flows according to dictated split ratios, but furthermore must resolve conflicts between multiple input flows which require the use of shared physical resources.

We therefore define a *phase* as a set of incoming links which can flow simultaneously through the node without causing resource conflicts. Each phase  $\psi$  for a node  $n$  is encoded as a sparse binary matrix of dimension  $|I_n| \times |O_n|$ , where element  $\psi_{l,m} = 1$  if link  $l$  is permitted to flow into link  $m$  as part of that phase (and otherwise 0). The set of all possible feasible phases for node  $n$  is denoted  $\Psi_n$ .

A flow-impeding signal controller is placed on each intersection node to ensure safe operation of the modeled junction by restricting concurrent flows across the node to those input links encoded in an element of  $\mathbf{G}_n \subset \Psi_n$ . Note that  $\mathbf{G}_n$  is generally limited to some subset of  $\Psi_n$  because practical signal controllers typically only actuate a limited number of phases due to hardware limitations or safety regulations. A controller on node  $n$  must alternate between actions  $G \in \mathbf{G}_n$  at an update rate dictated by management constraints or objectives.

Assume for now that all turn directions of a “shared movement” link are actuated simultaneously: if a node’s input link  $l$  is permitted to flow into any one of its downstream neighboring links  $m \in Out(l)$ , it is also permitted to flow into any of its other downstream neighbors. Then define  $G_l \in \{0, 1\}$  to be the indicator that link  $l$  is permitted to discharge according to its fixed expected split ratios.

Because links are defined to have finite storage capacity, nodes must also enforce physical limitations in flow due to congestion on their neighboring links. Flow through a node is therefore furthermore limited by two additional factors: the *sending constraints* of its upstream links, and the *receiving constraints* of its downstream links. Intuitively, the set  $\{S_l(t), l \in I_n\}$  of upstream sending constraints imposed on node  $n$  considers the number of vehicles currently available to be serviced by the node on each of its incoming links. The relevant downstream receiving constraints  $\{R_m(t), m \in O_n\}$  are limitations in the service rate of the node due to lack of space downstream to receive the transmitted flow.

The specific forms of  $S(t)$  and  $R(t)$  will vary according to the link dynamics being modeled. But in terms of these generalized constraints, the flow departing each upstream link  $l \in I_n$  can be defined as follows:

$$d_l(t) = G_l(t) \min \left\{ S_l(t), \min_{z \in Out(l)} \left\{ \frac{1}{\beta_n^{l,z}} R_z(t) \right\} \right\} \quad (3)$$

where  $n$  is the terminal node of link  $l$ . Notice that this is designed to enforce that vehicles follow a *first in, first out* (FIFO) principle: queue discharge is limited by the *most restrictive* downstream demand function so that downstream queue capacities are not exceeded while discharge remains consistent with the specified static split ratios. The flow arriving into downstream queues  $m \in O_n$  must then balance this departing flow:

$$a_m(t) = \sum_{k \in I_n} \beta_n^{k,m} d_k(t) \quad (4)$$

As previously mentioned, CTM and VCM impose different sending and receiving constraints on network nodes. These differences are related to the variations in how they depict congestion within a link. The remainder of this section describes the difference between these two model link dynamics.

### 5 Cell Transmission Model (CTM)

The CTM is a discrete-time finite difference scheme which numerically approximates the LWR hydrodynamic model of traffic flow. Define  $\rho(x, t)$  to be the density of vehicles at spatial location  $x$  and time  $t$ , and  $q(\rho)$  to be the corresponding flow of vehicles at point  $(x, t)$ . The LWR model is defined by the following flow-conserving partial differential equation:

$$\frac{\partial \rho}{\partial t} + \frac{\partial}{\partial x}(q(\rho)) = 0 \quad (5)$$

The discretization scheme of CTM specifically defines a piecewise-linear relationship between flow  $q$  and density  $\rho$ , an example of which is shown in Figure 2. For modeled link  $l$ , this *fundamental diagram* relationship is parameterized by free-flow velocity  $V_l$ , maximum (capacity) flow  $c_l$ , queue dissipation speed  $W_l$ , and maximum (jam) density  $\rho_l^{\max}$ :

$$q_l(\rho_l(x, t)) = \min \left\{ V_l \rho(x, t), c_l, W_l (\rho_l^{\max} - \rho_l(x, t)) \right\} \quad (6)$$

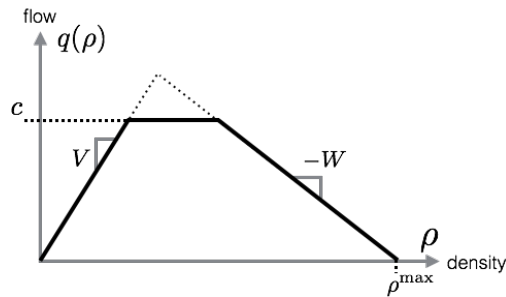


**FIGURE 2** The discretization scheme of CTM enforces a piecewise-linear relationship between the spatial density of vehicles on a link and the flow of vehicles through the link. A triangular variety in which  $\rho^{\max} = c \left( \frac{1}{V} + \frac{1}{W} \right)$  is also widely employed.

Consider a temporal discretization with uniform time steps of length that is small relative to typical actuation times for a signal control phases in the network being modeled. In CTM, a road is spatially discretized into a series of homogenous *cells* of uniform length which is equal to the distance traveled by free-flowing traffic in a single model time interval  $\Delta t$ . Each network link  $l$  is therefore divided into a series of  $\tau_l = \lfloor \frac{L_l}{V_l \cdot \Delta t} \rfloor$  cells. An illustration of this cell division is presented in Figure 3.

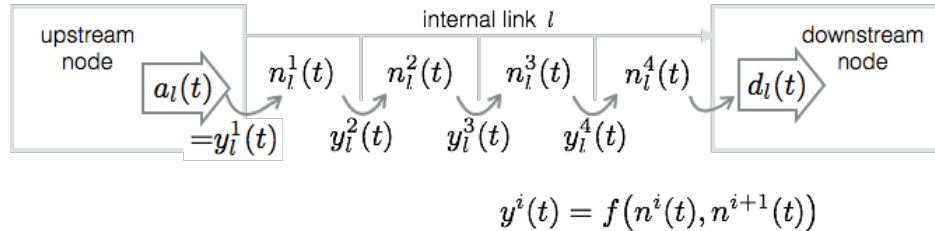


**FIGURE 3** At each CTM time step, cell state  $n^i(t)$  is increased by inflow  $y^i(t)$  and decreased by outflow  $y^{i+1}(t)$ . The state update equation for this cell is therefore a function of both the state of cell  $i$  and the state of the downstream cell  $i + 1$ . A link's receiving constraint  $R_l(t)$  is a function of only the first cell's state  $n_l^1(t)$ , and its sending constraint  $S_l(t)$  is a function of only the last cell's state  $n_l^{\tau_l}(t)$ .

Also define the following *cell-normalized* fundamental diagram parameters:

$$\begin{aligned}\tilde{\mathbf{V}}_l &= \mathbf{V}_l \cdot \frac{\Delta t \tau_l}{L_l} \\ \tilde{\mathbf{W}}_l &= \mathbf{W}_l \cdot \frac{\Delta t \tau_l}{L_l} \\ \tilde{c}_l &= c_l \Delta t \\ \tilde{N}_l &= \rho_l^{\max} \frac{L_l}{\tau_l}\end{aligned}$$

The state of each network link  $l$  can then be represented by a vector  $n_l$  with elements  $\{n_l^i, i = 1, \dots, \tau_l\}$  representing the vehicle-count in each of these sequential cells. These scaled density states evolve according to the vehicle conservation relationship

$$n_l^i(t+1) = n_l^i(t) + y_l^i(t) - y_l^{i+1}(t) \quad (7)$$

where  $y^i(t)$  represents the number of vehicles entering cell  $i$  during each time interval, defined as follows:

$$y^i(t) = \begin{cases} a_l(t), & i = 1 \\ \min \left\{ \tilde{\mathbf{V}}_l n_l^{i-1}(t), c_l, \tilde{\mathbf{W}}_l [\tilde{N}_l - n_l^i(t)] \right\} \nu_l \cdot \Delta t, & i = 2, \dots, \tau_l \\ d_l(t), & i = \tau_l + 1 \end{cases} \quad (8)$$

with  $\nu_l$  equal to the number of lanes on link  $l$ . The receiving constraint put on the upstream node of a CTM link is a function of the state of only the first cell in a link,  $n_l^1(t)$ :

$$R_l(t) = \nu_l \min \left\{ c_l, \tilde{\mathbf{W}}_l [\tilde{N}_l - n_l^1(t)] \right\} (\Delta t) \quad (9)$$

Similarly, the sending constraint put on a downstream node is a function of only the last cell's state  $n_l^{\tau_l}(t)$ :

$$S_l(t) = \nu_l \min \left\{ c_l, \tilde{\mathbf{V}}_l n_l^{\tau_l}(t) \right\} (\Delta t) \quad (10)$$

### Vertical Cell Model (VCM)

VCM is a new approach to a vertical queueing model which largely approximates the behavior of a point-queue model in the same cell-based context as CTM. Unlike most vertical queueing model formulations, it maintains a well-defined representation of both link travel delay and finite queue capacity. In this way, VCM may be classified as what some call a *spatial queueing model*.

Upon entering a VCM link, flows propagate at each step (without constraint) through a sequence of  $(\tau_l - 1)$  *transit cells*, after which they enter a terminal *queueing cell*. Therefore  $\tau_l = \lfloor \frac{L_l}{V_l \cdot \Delta t} \rfloor$  state variables are required to represent the state of each link  $l$  in VCM (as in CTM):

- $v_l^i(t)$ ,  $i = 1, \dots, (\tau_l - 1)$  are non-negative values representing the amount of vehicle-flow that has entered the link at time  $t - i$ , but has not yet traveled the length of the link to become eligible to exit, and
- $q_l(t)$  represents the amount of vehicle-flow which has traversed the entire link length and is therefore queued to immediately exit the link.

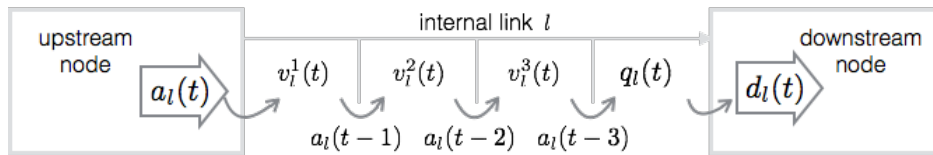


**FIGURE 4** VCM passes link input flows a constant rate between non-physical “transit cells” until they reach a vertical “exit queue”. To enforce finite queue storage capacity, link receiving constants are a function of the number of vehicles in all “cells” of the network. Sending constraints, however, only depend on the number of vehicles that are explicitly in the exit queue.

Explicitly, the transit queue states  $v_l^i(t)$  and exit queue state  $q_l(t)$  evolve as follows:

$$\begin{bmatrix} v_l^1(t+1) \\ v_l^2(t+1) \\ v_l^3(t+1) \\ \vdots \\ v_l^{\tau_l-2}(t+1) \\ v_l^{\tau_l-1}(t+1) \\ q_l(t+1) \end{bmatrix} = \begin{bmatrix} 0 & 0 & 0 & \dots & 0 & 0 & 0 \\ 1 & 0 & 0 & \dots & 0 & 0 & 0 \\ 0 & 1 & 0 & \dots & 0 & 0 & 0 \\ \vdots & \vdots & \ddots & \ddots & \vdots & \vdots & \vdots \\ 0 & 0 & 0 & \dots & 0 & 0 & 0 \\ 0 & 0 & 0 & \dots & 1 & 0 & 0 \\ 0 & 0 & 0 & \dots & 0 & 1 & 1 \end{bmatrix} \begin{bmatrix} v_l^1(t) \\ v_l^2(t) \\ v_l^3(t) \\ \vdots \\ v_l^{\tau_l-2}(t) \\ v_l^{\tau_l-1}(t) \\ q_l(t) \end{bmatrix} + \begin{bmatrix} 1 & 0 \\ 0 & 0 \\ 0 & 0 \\ \vdots & \vdots \\ 0 & 0 \\ 0 & 0 \\ 0 & -1 \end{bmatrix} \begin{bmatrix} a_l(t) \\ d_l(t) \end{bmatrix} \quad (11)$$

This progression of vehicles across a VCM link is also illustrated in Figure 4.

Each VCM link is parameterized by a freeflow travel velocity  $V_l$ , a maximum flow rate (capacity)  $c_l$ , and a fixed queue capacity (per lane)  $\kappa_l$ . Notably, however, VCM links do not enforce a fundamental relationship between spatial density and flow rate. Unlike the independent cell supply limitation of CTM, receiving constraints in VCM are a function of the state of all link cells:

$$R_l(t) = v_l \min \left\{ c_l \cdot \Delta t, \kappa_l - q_l(t) - \sum_{i=1 \dots (\tau_l-1)} v_l^i(t) \right\} \quad (12)$$

VCM sending constraints, however, depend only on vehicles that are explicitly in the exit queue:

$$S_l(t) = \nu_l \min \{c_l \cdot \Delta t, q_l(t)\} \quad (13)$$

### Interpretation of the Physical Differences Between VCM and CTM

The independent storage capacity constraints of cells within a CTM link propagates the spatial location of high-density flows within a road link. This characterizes a *horizontal* queueing model. Such spatial differentiation is a theoretically desirable characteristic, especially for representing  
 5 freeways or major highways with long spans where flow is not artificially interrupted. While CTM should be able to propagate the effects of the theoretical “stop and go” shockwaves created by frequent stopping due to signal controllers, accurate representation of these types of behaviors would necessitate extremely high spatial resolution and therefore high temporal discretization in a CTM implementation (recall that  $\tau_l = \lfloor \frac{L_l}{V_l \cdot \Delta t} \rfloor$ ).

10 Meanwhile, network cells on an arterial road corresponding to a model time step of 1-5 seconds typically represent very small portions of roadway where the relationship between flow and density is not always as well-defined. As can be seen in a visualization of observed vehicle trajectories on an urban network (available online at <http://youtu.be/jJen2ybNr34>), queue aggregation and dissipation behaviors can vary significantly from link to link. Hence tuning the required funda-  
 15 mental diagram parameters to precisely represent observed conditions is a challenge—especially the backwards shockwave speed  $W$ , which is even difficult to measure will full knowledge of system state. Furthermore, queues do not always dissipate as would be predicted by a rigid fundamental diagram relationship. This is perhaps because unmodeled factors such as varying driver response and vehicle acceleration times are dominant in practical urban traffic dynamics.

20 Unlike the horizontal queue of CTM, VCM models a *vertical queue* or “stack” which is not assigned to any physical distance along the link. It can be interpreted as modeling vehicles that can only either travel at maximum velocity ( $V$ ) or be completely stopped. These vehicles traverse the entire distance of a link, unconstrained by downstream congestion, before stopping in a queue. Hence flow across a VCM link is less constrained by the presence of congestion. Furthermore,  
 25 queue dissipation is not limited by shockwave speed  $W$  in VCM as it is in CTM. Instead, link flow capacity is the only constraint on queue discharge. It is therefore expected that link queues may empty more quickly in VCM than in CTM.

Another effect of the vertical queueing approach is the difference in upstream receiving (or supply) constraints. A downstream departure will immediately yield effects on link receiving  
 30 constraints in VCM, while the effect of departures will take at least  $\tau$  time steps to impact receiving constraints in CTM. The physical representativeness of this behavior remains to be examined, but it will depend on the synchronization of a link’s service periods to demand patterns caused by upstream signals.

These two simplifications of VCM (as compared to CTM) result in the linear model for link  
 35 dynamics shown in equation (11). In fact, the only non-linearities in VCM are contained within the network node model. The linear link model yields potential benefits for the derivation of link-state estimation and model-based control procedures.

### VALIDATION PROCEDURE

40 Our experimental network was designed to simulate the flows on five blocks of Lankershim Blvd. in Los Angeles, California, USA. The selection of this simulation area was motivated by the avail-



A visual inspection of the data in the form of an animated compilation of vehicle trajectories, available online at <http://youtu.be/jJen2ybNr34>, reveals that flows were typically constrained only by signal controllers: vehicles did not suffer severe delays due to pedestrians or other uncontrolled obstacles.

5 Due to the priority put on the through movements of the signals on Lankershim Blvd in the relevant signal control parameters, the observed links were generally undersaturated throughout the entire observation period. However some oversaturation caused noticeable congestion from Link 2NB to spill back onto Link 1NB during the last ten minutes of data collection. Unfortunately, the effects of this spillback on link 1NB were unobservable due to the limited geographical range of  
10 the trajectory data (very few of the vehicles originating from Link 1 were detected to be on the link in the trajectory data).

To specifically evaluate both VCM and CTM, we compared the output densities and flows output by each model to the observed density and flow patterns generated by aggregating the positions documented in the tracked trajectories over time and space. Both models were implemented  
15 using the *Berkeley Advance Traffic Simulation* (BeATS) platform with a model discretization of  $\Delta t = 1$  second. They shared a common graphical network (shown in Figure 5) and were initialized with the same geometric information, input flows, split ratios, and signal timings.

Geometry data such as link length and lane count was compiled from a satellite map image and various NGSIM documentation. The network graph used in this procedure is illustrated in  
20 Figure 5. Incoming boundary flows were collected by aggregating the initial appearances of tracked vehicles at each entry link with a five second resolution. Split ratios were considered static over the entire simulation period. They were estimated by comparing the vehicle counts corresponding to each intersection approach aggregated over the entire observation period. Signal parameters were documented in the NGSIM data package, but we synchronized the precise offsets to correspond  
25 to trajectory data timestamps via the initiation of observed outflows in links corresponding to the major approaches for each intersection.

## RESULTS

Both VCM and CTM were able to accurately predict the general levels of congestion observed on the Lankershim Blvd network during the 30 minute observation period with minimal parameter  
30 tuning. In fact, we found only minute differences in the modeled link outflows for the entire period of available data. Both models seemed to smooth “spikes” in the true link outflows, which were most likely physically caused by unpredictable variations in driver acceleration behaviors. When differences in modeled outflows did exist, the most common observation was that CTM seemed to attenuate the observed outflows at a slightly higher magnitude, as seen in the example in Figure 6.  
35 This could be caused by the delay on queue dissipation imposed by the dissipation wave speed  $W$  in CTM’s flow-density relation: modeled flows are constrained in a queue slightly longer and at a location further upstream in CTM than in VCM, where the exit queue is only limited by link flow capacity and it is assumed that the travel time of de-queuing vehicles has already been incurred.

The errors observed in all modeled link outflows, as shown in Figure 7, reveal little vari-  
40 ation between the errors in outflows predicted by the two link dynamics. But by analyzing cumulative modeled link outflows, it becomes apparent that both models have a slight tendency to overestimate links outflows. The percent of cumulative error in outflow estimates for all through-movements on Lankershim Blvd. links over the entire simulation period are tabulated in Table 1. The similarity between the cumulative outflow estimation errors of the two models suggests that

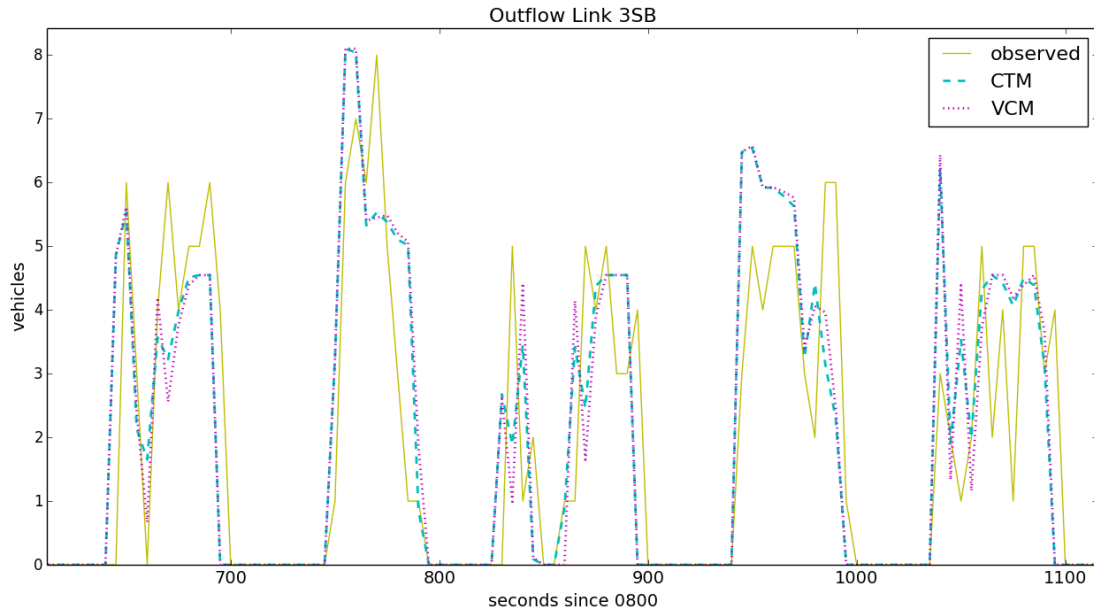


**FIGURE 6** Modeled and observed flows exiting the through movement of Link 3 in the southbound direction illustrate typical outflow variations in this analysis. Both models seemed to smooth the true outflows, but reached approximated capacity flows at similar times.

this error was more likely caused by unpredictable flow impediments, parameter mistuning, or a common misrepresentation in the network geometry than by differences in fundamental modeling assumptions.

**TABLE 1** Cumulative Outflow Model Error

Model Type	Link 2NB	Link 3NB	Link 4NB	Link 4SB	Link 3SB	Link 2SB
CTM	0.93%	4.53%	1.69%	0.79%	9.25%	6.74%
VCM	0.84%	4.29%	1.27%	0.76%	9.09%	6.53%

As expected given the similarities between link flow transfers, CTM and VCM yielded very similar link-vehicle counts aggregated over a 5-second time period. The modeled and observed states of all internal network links representing through movements are depicted in Figure 8. While VCM typically resulted in slightly larger link densities than CTM, it was not necessarily more representative of true link state. Neither model seemed to have a clear advantage over the other in correctly estimating link state.

## CONCLUSION

Our results serve to validate the use of a vertical queuing model such as VCM in the case of the studied network. In fact, in our analysis (which was limited to a single model run by the lack of appropriate data), VCM appears to have performed slightly better than CTM in terms of cumulative link flow error. This work may help justify the relative analytical simplicity of using a similar point queue dynamics for applications of model-based arterial estimation and signal control—especially

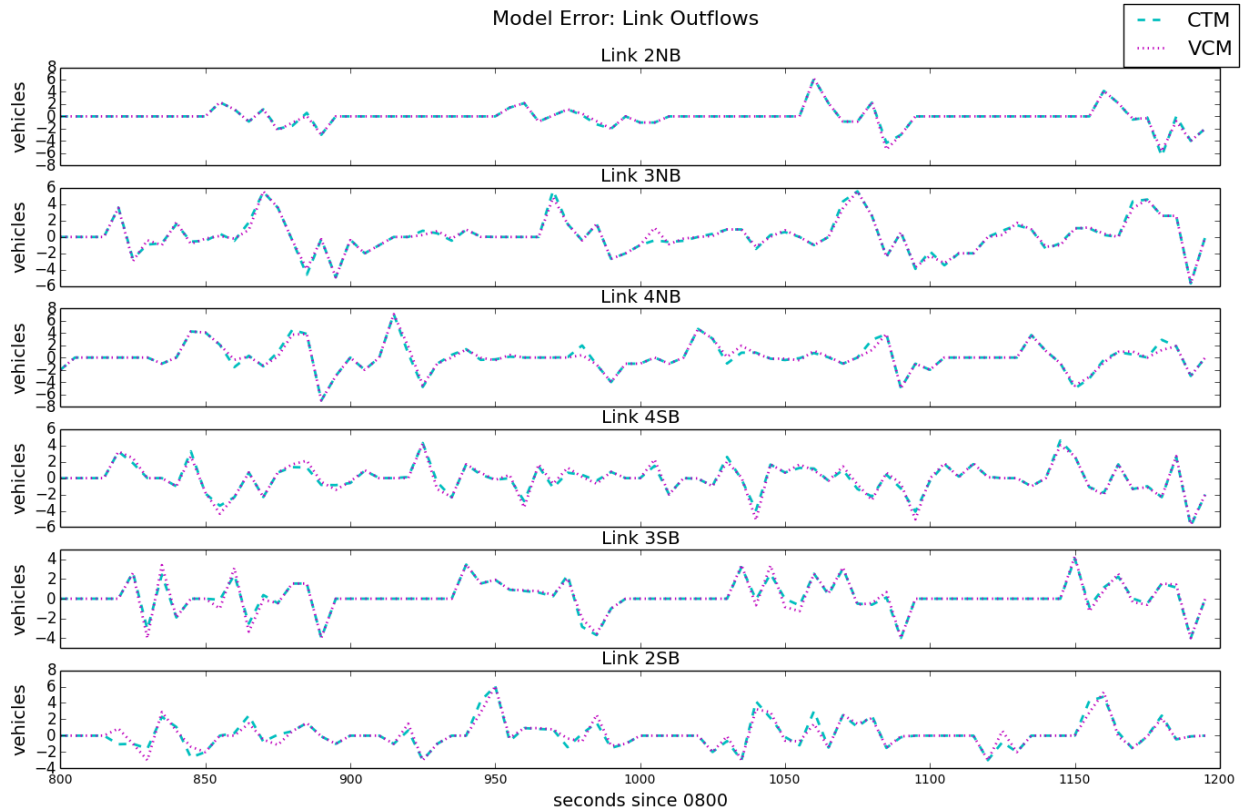


**FIGURE 7 Differences in link outflow error between CTM and VCM (relative to observation) were minimal.**

in cases where the measurements available for controller feedback is of very low resolution.

Because the links on Lankershim Blvd remained in the undersaturated regime for the entire observation period, we were notably not able to investigate model performance in the high-congestion conditions where CTM is expected to out-perform a vertical model. Likely due to this lack of over-saturation, we also found very little output sensitivity to backwards shockwave speed  $W$  in the CTM model—which is the critical difference in the assumptions of CTM and VCM. This unfortunately prevented conclusive results on the relative benefits of a horizontal queueing model.

Yet further analysis is limited by the lack of quality ground truth data on an appropriate urban network. We plan to immediately repeat this procedure with the companion NGSIM arterial trajectory data set on Peachtree St. in Atlanta. This network features longer links with more volume but lower velocities.

We also seek opportunities to compare the estimations provided by each of these models to a calibrated microsimulation model of a congested network with high connectivity. We would like to quantify the network impacts of congestion on a grid-link network with the possibility of complicated routing patterns and more significant conflicting flow demands. However, the most difficult part of this investigation was the formalization of a network representation that could accurately capture all of the characteristics of a realistic traffic network, including capacity reductions from turn bay blocking and complete independence of non-simultaneously-actuated queues. A larger or more inter-connected network would intensify this part of the modeling procedure.

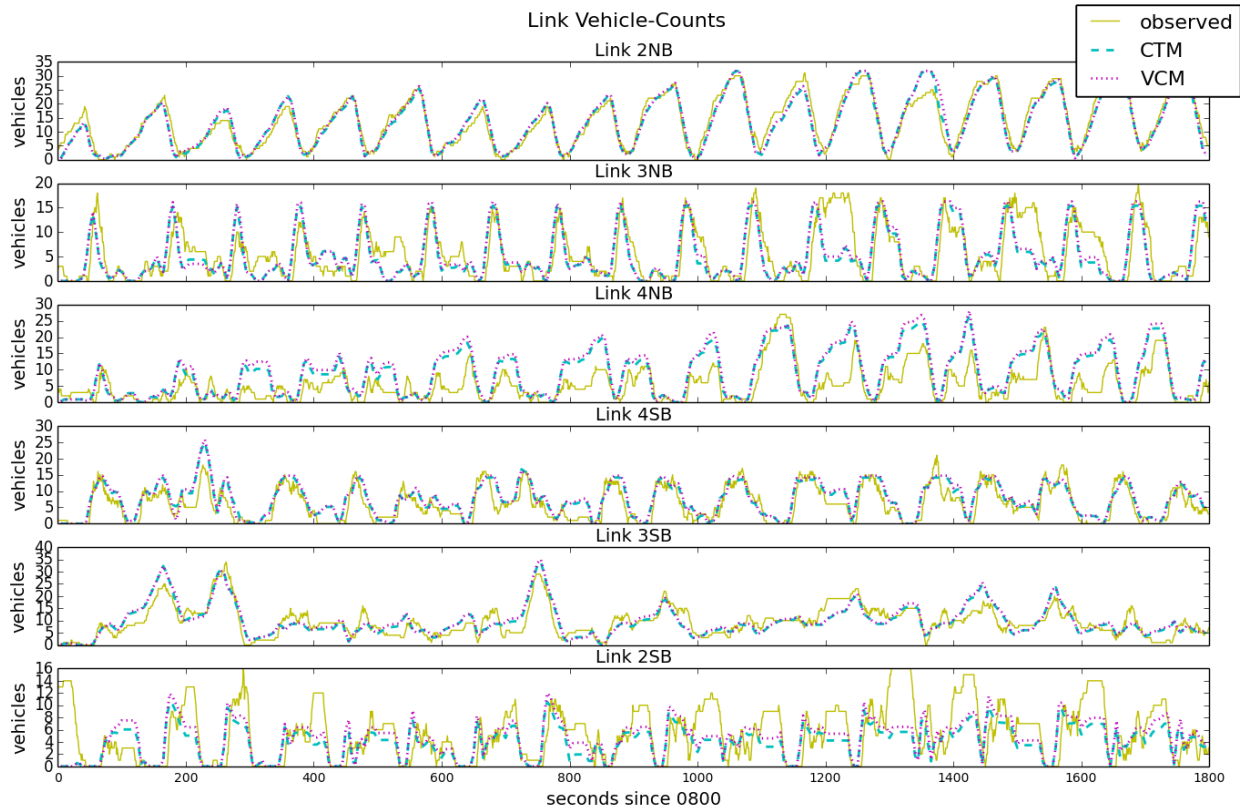


**FIGURE 8** The modeled flow differences resulted in minor variations in link density states in the internal links, but neither model consistently resulted in a better representation of link state.

While VCM is analytically simpler than a horizontal queueing model and results in different queue dissipation behaviors, it does not provide any computational benefit over a CTM that is run at the same time discretization. We are currently developing a generalized analytical point queue model which could be implemented on a simplified arterial graphical network. In future work we will propose a link dynamics which will eliminate the need for explicit representation of parallel “movement” links in the underlying network structure. Instead, separate capacities on co-located movement queues will be tracked within the mathematical structure of the vertical queueing model. This would greatly simplify the process of building an appropriate representative network structure (which is a significant obstacle to a practical implementation of such a queueing model).

We ultimately hope to deploy an appropriate queueing model of an arterial network surrounding the I-210 freeway near Los Angeles, California as part of California PATH’s *Connected Corridors* integrated corridor management project (<http://connected-corridors.berkeley.edu/>). We seek a model of dynamic traffic flow that is easily tunable and practical for largely-automated functionality, but is also sufficiently accurate on realistic urban networks to produce estimations for use in predictive control procedures. Additionally, we want our selected model to be easily interfaced with a concurrent macroscopic freeway model in terms of shared boundary flows and equivalent calculations of performance metrics.

## ACKNOWLEDGEMENT

The high-resolution trajectory data set used in this study was collected and provided by the Next Generation Simulation Community. This work was funded by the California Department of Transportation under the Connected Corridors program at California PATH.

## 5 REFERENCES

- [1] Gazis, D. C. and R. B. Potts, The oversaturated intersection. In *2nd International Symposium on the Theory of Road Traffic Flow*. Organization for Economic Cooperation and Development, Paris, 1963, pp. 221–237.
- [2] Gazis, D. C. Optimum Control of a System of Oversaturated Intersections. *Operations Research*, Vol. 12, No. 6, 1964, pp. 815–831.
- [3] Gazis, D. C. Modeling and optimal control of congested transportation systems. *Networks*, Vol. 4, 1974, pp. 113–124.
- [4] Singh, M. G. and H. Tamura. Modelling and hierarchical optimization for oversaturated urban road traffic networks. *International Journal of Control*, Vol. 20, No. 6, 1974, pp. 913–934.
- [5] D’Ans, G. C. and D. C. Gazis. Optimal control of oversaturated store-and-forward transportation networks. *Transportation Science*, Vol. 10, No. 1, 1976, pp. 1–19.
- [6] Park, E. S., J. H. Lim, I. H. Suh, and Z. Bien. Hierarchical optimal control of urban traffic networks. *International Journal of Control*, Vol. 40, No. 4, 1984, pp. 813–829.
- [7] Michalopoulos, P. G. and G. Stephanopoulos. Oversaturated signal systems with queue length constraints—II: Systems of intersections. *Transportation Research*, Vol. 11, 1977, pp. 423–428.
- [8] Lighthill, M. J. and G. B. Whitham. On Kinematic Waves. II. A Theory of Traffic Flow on Long Crowded Roads. *Proceedings of the Royal Society of London. Series A. Mathematical and Physical Sciences*, Vol. 229, No. 1178, 1955, pp. 317–345.
- [9] Richards, P. I. Shock Waves on the Highway. *Operations Research*, Vol. 4, No. 1, 1956, pp. 42–51.
- [10] Stephanopoulos, G. and P. G. Michalopoulos. Modelling and analysis of traffic queue dynamics at signalized intersections. *Transportation Research Part A: Policy and Practice*, Vol. 13, No. 5, 1979, pp. 295–307.
- [11] Daganzo, C. F. The cell transmission model: A dynamic representation of highway traffic consistent with the hydrodynamic theory. *Transportation Research Part B: Methodological*, Vol. 28B, No. 4, 1994, pp. 296–287.
- [12] Daganzo, C. F. The cell transmission model, part II: network traffic. *Transportation Research Part B: Methodological*, Vol. 29B, 1995, pp. 79–93.

- [13] Smilowitz, K. R. and C. Daganzo, *Predictability of Time-dependent Traffic Backups and Other Reproducible Traits in Experimental Highway Data*. UCB-ITS-PWP-99-5, California PATH, 1999.
- [14] Smilowitz, K. R., C. F. Daganzo, and M. J. Cassidy. Some observations of highway traffic in long queues. *Transportation Research Record: Journal of the Transportation Research Board*, Vol. 1678, No. 1, 1999, pp. 225–233.
- [15] Zhang, H. M., Y. M. Nie, and Z. S. Qian. Modelling network flow with and without link interactions: the cases of point queue, spatial queue and cell transmission model. *Transportmetrica B: Transport Dynamics*, Vol. 1, No. 1, 2013, pp. 33–51.
- [16] Gomes, G. and R. Horowitz. Optimal freeway ramp metering using the asymmetric cell transmission model. *Transportation Research Part C: Emerging Technologies*, Vol. 14, No. 4, 2006, pp. 244–262.
- [17] Maher, M. A comparison of the use of the cell transmission and platoon dispersion models in TRANSYT 13. *Transportation Planning and Technology*, Vol. 34, No. 1, 2011, pp. 71–85.
- [18] Gomes, G., R. Horowitz, A. A. Kurzhanskiy, P. P. Varaiya, and J. Kwon. Behavior of the cell transmission model and effectiveness of ramp metering. *Transportation Research Part C: Emerging Technologies*, Vol. 16, No. 4, 2008, pp. 485–513.
- [19] Abu-Lebdeh, G. and R. F. Benekohal. Development of traffic control and queue management procedures for oversaturated arterials. *Transportation Research Record: Journal of the Transportation Research Board*, Vol. 1603, 1997, pp. 119–127.
- [20] De Schutter, B. and B. De Moor. Optimal Traffic Light Control for a Single Intersection. *European Journal of Control*, Vol. 4, No. 3, 1998, pp. 260–276.
- [21] Lo, H. K. A cell-based traffic control formulation: strategies and benefits of dynamic timing plans. *Transportation Science*, Vol. 35, No. 2, 2001, pp. 148–164.
- [22] Lin, W. H. and C. Wang. An Enhanced 0-1 Mixed-Integer LP Formulation for Traffic Signal Control. *IEEE Transactions on Intelligent Transportation Systems*, Vol. 5, No. 4, 2004, pp. 238–245.
- [23] Beard, C. and A. Ziliaskopoulos. System optimal signal optimization formulation. *Transportation Research Record: Journal of the Transportation Research Board*, Vol. 1978, 2006, pp. 102–112.
- [24] Aboudolas, K., M. Papageorgiou, and E. Kosmatopoulos. Store-and-forward based methods for the signal control problem in large-scale congested urban networks. *Transportation Research Part C: Emerging Technologies*, Vol. 17, 2009, pp. 163–174.
- [25] Kashani, H. R. and G. N. Saridis. Intelligent Control for Urban Traffic Systems. *Automatica*, Vol. 19, No. 2, 1983, pp. 191–197.

- [26] Davison, E. J. and U. Ozguner. Decentralized control of traffic networks. *IEEE Transactions on Systems, Man, and Cybernetics*, Vol. SMC-13, No. 4, 1983, pp. 476–487.
- [27] Papageorgiou, M. An integrated control approach for traffic corridors. *Transportation Research Part C: Emerging Technologies*, Vol. 3, No. 1, 1995, pp. 19–30.
- 5 [28] Wey, W. M. and R. Jayakrishnan. Network traffic signal optimization formulation with embedded platoon dispersion simulation. *Transportation Research Record: Journal of the Transportation Research Board*, Vol. 1683, 1999, pp. 150–159.
- [29] Diakaki, C., M. Papageorgiou, and K. Aboudolas. A multivariable regulator approach to traffic-responsive network-wide signal control. *Control Engineering Practice*, Vol. 10, No. 2, 10 2002, pp. 183–195.
- [30] van den Berg, M., A. Hegyi, and B. De Schutter. Integrated traffic control for mixed urban and freeway networks: A model predictive control approach. *European Journal of Transport and Infrastructure Research*, Vol. 7, 2007, pp. 223–250.
- [31] Lin, S. and Y. Xi, An Efficient Model for Urban Traffic Network Control. In *th World Congress of the International Federation of Automatic Control*, 2008, pp. 14066–14071. 15
- [32] Aboudolas, K., M. Papageorgiou, and A. Kouvelas. A rolling-horizon quadratic-programming approach to the signal control problem in large-scale congested urban road networks. *Transportation Research Part C: Emerging Technologies*, Vol. 18, 2010, pp. 680–694.
- 20 [33] Wongpiromsarn, T., T. Uthaicharoenpong, Y. Wang, E. Frazzoli, and D. Wang, Distributed traffic signal control for maximum network throughput. In *15th International IEEE Conference on Intelligent Transportation Systems*. IEEE, 2012, pp. 588–595.
- [34] Varaiya, P. P. Max pressure control of a network of signalized intersections. *Transportation Research Part C: Emerging Technologies*, Vol. 36, 2013, pp. 1–19.